Comparison of registration strategies for USCT-MRI image fusion: preliminary results

T. Hopp, P. Cotic Smole, and N.V. Ruiter

Karlsruhe Institute of Technology, Institute for Data Processing and Electronics, Karlsruhe, Germany
E-mail: torsten.hopp@kit.edu

Abstract

Comparing Ultrasound Computer Tomography (USCT) to the well-known Magnetic Resonance Imaging (MRI) is an essential step in evaluating the clinical value of USCT. Yet the different conditions of the breast either embedded in water (USCT) or in air (MRI) prevent direct comparison. In this work we compare two strategies for image registration based on biomechanical modeling to automatically establish spatial correspondence: a) by applying buoyancy to the MRI, or b) by removing buoyancy from the USCT. The registration was applied to 9 datasets from 8 patients. Both registration strategies revealed similar registration accuracies (MRI to USCT: mean = 5.6 mm, median = 5.6 mm, USCT to MRI: mean = 6.6 mm, median = 5.7 mm). Image registration of USCT and MRI allows to delineate corresponding tissue structures in both modalities in the same or nearby slices. Our preliminary results indicate that both simulation strategies seem to perform similarly. Yet the newly developed deformation of the USCT volume is less computationally demanding: As the breast is subjected to buoyancy it can thereby serve as the unloaded state while for the contrary strategy we have to solve an inverse problem.

Keywords: Image registration, Biomechanical breast model, Ultrasound Computer Tomography, Magnetic Resonance Imaging

1 Introduction

Among other Ultrasound Computer Tomography (USCT) systems, e.g. [1, 2], KIT's full 3D USCT system is currently being tested in clinical trials [3]. In this development state of a novel imaging modality it is essential to correlate the images to well-known imaging modalities in order to learn the imaging characteristics and evaluate the diagnostic value of USCT. In our clinical studies we use Magnetic Resonance Imaging (MRI) as a three-dimensional modality of choice for comparison to 3D USCT images. Yet the different environmental conditions of

the breast either embedded in water (USCT) or in air (MRI) and the contact of the breast with the MRI breast coils lead to different non-linear deformations of the breast in 3D, which result in a challenging correlation of tissue structures.

In our previous work [4] we presented an automated image registration method to overcome these considerable differences during the image acquisition. The challenging non-linear deformations of the soft tissue are tackled by applying patient-specific biomechanical breast models. The models are until now generated based on the MRI volumes and the registration process simulates the effect of buoyancy to create deformed MRI volumes which are directly comparable to the USCT volume. The buoyancy simulation is approximated by estimating the unloaded state of the breast, i.e. to remove the gravity that is acting on the breast during MRI acquisition. Hence we have to solve an inverse problem of estimating the unknown unloaded state from a loaded state, which can be derived by an iterative procedure [5] and is therefore time consuming. In this work we consider the opposite strategy: deforming the breast imaged in USCT to match the breast shape in the MRI. Due to assuming the breast imaged in USCT as the approximate unloaded state this might be beneficial for biomechanical modeling as only the forward problem of applying gravity has to be solved. This papers describes the developed methods and presents the preliminary results comparing both registration strategies.

2 Methods

The key difference between USCT and MRI is the breast positioning in water respectively air. In particular the gravity which is present during MRI acquisition causes an elongation of the breast in anteroposterior direction and a contraction in mediolateral respectively craniocaudal direction. In contrast, the breast shape during USCT image acquisition approximately equals the gravity-free state as buoyancy and gravity are in equilibrium. In our previous approach - here denoted as strategy A - the general idea is to simulate the buoyancy effect by estimating the gravity-free state of the breast from the MRI (Figure 1). In the new approach - here denoted as strategy B - the breast imaged in USCT is assumed to be in a gravity-free state and we simulate the gravity effect (Figure 2). For both strategies we apply patient-specific biomechanical models and Finite Element simulations to estimate the large deformation. Following the biomechanical model based deformation, a cubic B-spline based free form deformation is applied to refine the surface overlap of the breasts in MRI and USCT respectively. Both registration steps rely on the breast surfaces detected in MRI and USCT images and do not consider additional landmarks to drive the registration.

A biomechanical model is constructed from the segmented MRI (strategy A) or USCT (strategy B) volume. The MRI based model requires a preprocessing of the MRI volume which includes a segmentation of the breast from the background using an automated state of the art segmentation method based on fuzzy C-means clustering [6]. As the MRI volume contains a whole cross-section of the patients body which is not relevant for the breast image registration, the volume is cropped at the sternum in anteroposterior direction, which is detected

automatically from the image. Furthermore the volume is resampled to an isotropic voxel size by a linear interpolation to overcome the gap between slices. The USCT based model is constructed by segmenting the breast from the background using a semi-automated edge detection and surface fitting approach [7].

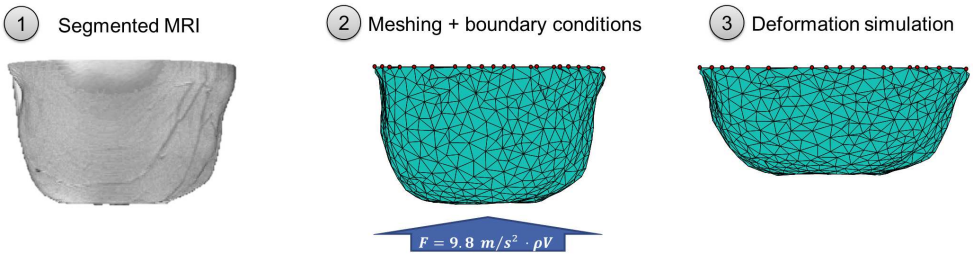

Figure 1: Illustration of image registration strategy A: a buoyancy simulation is applied to the breast acquired in MRI to obtain the loading configuration of the breast during imaging in USCT. Note that the illustration refers to the simplified buoyancy simulation using a simple body load. For the full resolution simulation an iterative approach is applied: a gravity load is applied iteratively and the estimate of the node positions in the unloaded state are updated to solve the inverse problem.

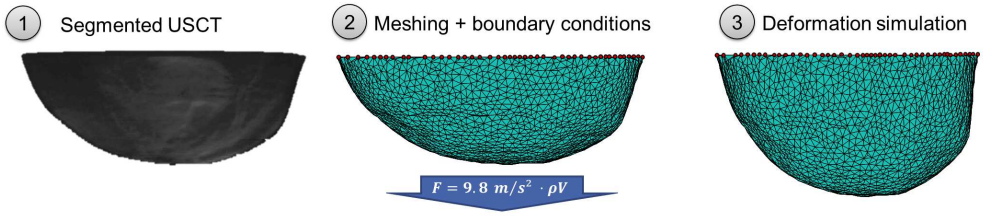

Figure 2: Illustration of image registration strategy B: a gravity simulation is applied to the breast acquired in USCT to obtain the gravity loaded configuration of the breast during prone MRI acquisition

The geometry of the biomechanical models is generated by a meshing algorithm [8] using 4-node tetrahedrons. A hyperelastic neo-hookean material model is applied. The breast tissue is assumed to be nearly incompressible by applying a Poissons ratio of 0.49. The material stiffness parameters, i.e. the Young's modulus E for fatty tissue (E_{FAT}), are initially applied constant for all patients. They are converted to the neo-hookean material constants using the relationship between the Young's modulus and the shear and bulk modulus as described in e.g. *Bower* [9].

Buoyancy is simulated by applying a body load with an acceleration of $g = 9.81\,m/s^2$, in posterior direction on the entire breast while posterior-most nodes of the mesh are held in position to model the fixation of the breast at the chest wall (strategy A). The resulting force F is given by $F = mg$ with m the mass of the water replaced by the breast volume V, i.e. $m = \rho V$ with the density of water $\rho = 1000\,kg/m^3$. Gravity is simulated vice versa: a body load is applied in anterior direction on the entire model assuming an average density of the breast of $\rho = 1000\,kg/m^3$, while posterior-most nodes are fixed (strategy B). To compute the biomechanical simulation, the commercial Finite Element Method (FEM) package ABAQUS [10] is used.

To enable a patient-specific registration, the material stiffness parameters as well as dataset rotation and cropping are automatically optimized using simulated annealing with bound constraints. The optimization criterion is the surface agreement between the deformed breast after buoyancy respectively gravity simulation and the corresponding breast in the USCT respectively MRI volume. The surface agreement is calculated as the average distance of closest points on both breast surfaces, which becomes minimal for perfectly overlapping breast images. An empirically chosen maximum of 50 iterations is used as a stopping criterion.

The image resolution of datasets included in this study was $(0.75\,mm)^3$ for the USCT volume and $0.91\,mm \times 0.91\,mm \times 3.0\,mm$ for the MRI volume. To accelerate the overall registration process, the parameter optimization is performed on images downsampled by factor two. After the optimization of the material parameters, the cropping and the rotation, the optimized parameters are used for a simulation in full resolution. In the case of strategy A, an iterative simulation similar to *Carter et al.*[5] to approximate the true unloaded state of the breast is applied for the full resolution simulation.

Due to simplifications of the biomechanical model compared to the unknown real biomechanics of the breast such as neglecting connective tissue structures like Cooper ligaments [11], the deformed images usually do not fully overlap. Furthermore the predeformation caused by a possible contact between the breast and the MRI breast coil may cause additional differences in the breast shape. Therefore an additional simulation step is performed to bring the MRI and USCT volumes in full overlap. The deformed MRI (strategy A) respectively deformed USCT (strategy B) after biomechanical simulation is rigidly aligned with the contrary modality based on both centers of mass in mediolateral direction and the chest wall in anteroposterior direction. Afterwards a 3D free form deformation with cubic B-splines is applied [12]. Again the surface agreement of deformed MRI and USCT is used as a penalty function for the optimization process that drives the free form deformation. Supporting grid point distances of the B-splines were manually chosen as a tradeoff between the local and global deformation of the breast.

To measure the accuracy of the registration, landmarks like lesions, predominant connective tissue structures or breast implants which could be clearly delineated in MRI as well as in USCT, were manually annotated in the unregistered MRI and the USCT volume by circumscribing the border of the structure with a freehand tool in 3D. The Target Registration Error (TRE) is defined as the average of Euclidean distances of closest points between the annotations in the unregistered and the compared modality.

3 Results

The registration was applied to nine datasets from eight patients of our first clinical study with the KIT 3D USCT [3]. The datasets were chosen such that at least one correlating tissue structure could be clearly delineated in one USCT volume and the MRI volume before the registration was carried out. In total 11 correlating tissue structures were annotated. In case of more than one marking in a breast the TRE was averaged for the particular volume image to estimate an error per registered dataset.

The TRE was analyzed for all processing steps:

(1) before the registration was carried out, i.e. applying a matching of the amount of tissue present in both images as well as a three-dimensional rigid alignment.

(2) after the buoyancy respectively gravity simulation was carried out.

(3) using the final registered state after applying the buoyancy respectively gravity simulation and the surface-refinement by the free form deformation.

The mean TRE before the registration was carried out (analysis 1) was 9.7 *mm* (median: 7.2 *mm*, standard deviation SD: 7.3 *mm*) for strategy A and 9.9 *mm* (median: 7.4 *mm*, standard deviation SD: 7.6 *mm*) for strategy B. The slight difference is due to the search for the closest point on the contrary modality.

When applying the buoyancy simulation in strategy A, the mean TRE reduces to 6.9 *mm* (median: 6.5 *mm*, SD: 2.7 *mm*). In contrary the strategy B reduces the TRE to an average of 7.9 *mm* (median: 5.9 *mm*, SD: 4.2 *mm*) when applying the gravity simulation.

After performing the additional surface-refinement by the free-form deformation, the average TRE for strategy A was 5.6 *mm* (median: 5.6 *mm*, SD: 2.4 *mm*) and the average TRE for strategy B was 6.6 *mm* (median: 5.6 *mm*, SD 4.0 *mm*).

Both registration strategies revealed similar registration accuracies. Compared to the simple alignment of datasets (analysis 1) the TRE is reduced by nearly factor 2 (analysis 3). Figures 3 and 4 show the registration results for the same patient for strategy A and strategy B respectively.

The parameter optimization resulted in similar average material stiffnesses for both registration strategies: the average E_{FAT} was 1792 *Pa* (median: 2172 *Pa*, SD: 794 *Pa*) for strategy A and 1853 *Pa* (median: 1200 *Pa*, SD: 1318 *Pa*) for strategy B.

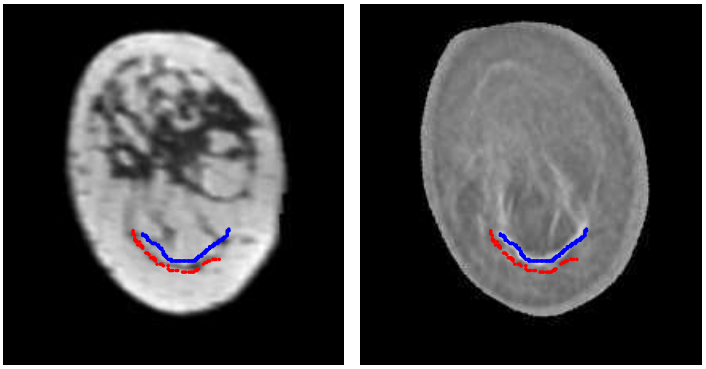

Figure 3: Result of the registration with strategy A. MRI (left) and USCT (right), each with markings of a connective tissue structure, which served as a basis for evaluation of the TRE. Blue denotes the surface points of the marking in USCT, red denotes the surface points of the marking in MRI. Note that both images show the same coronal slice from the 3D volumes.

4 Discussion and conclusion

Our proposed registration method is aimed at improving visual and quantitative comparison of tissue structures in USCT and MRI as it spatially correlates the images of both modalities automatically. We previously successfully developed, applied and evaluated a method for registration of MRI and USCT volumes which allows to delineate corresponding tissue structures more easily [4]. In this paper we preliminarily evaluated two registration strategies: either simulating the buoyancy effect to deform the MRI or removing the buoyancy effect to deform the USCT.

Both strategies lead to similar results with respect to the TRE. The previous method (strategy A) results in a slightly lower average TRE when using only the biomechanical model simulation without the additional surface-refinement by the free-form deformation (analysis 2), however the median values are comparable, i.e. there is only one outlier which causes the increase in the average TRE. With both strategies the median TREs vary by max. $0.6\,mm$ in all analyzed processing steps. A limitation of the current study is the low number of datasets, which limits the analysis of statistical significance of the results. Furthermore the experiments were carried out with simplified homogeneous biomechanical models, which do not distinguish between different types of tissue within the breast. In a future analysis we are planning to test more sophisticated models, e.g. similar to *Cotic Smole et al.* [13] for strategy A or similar to *Hopp et al.* [14] for strategy B.

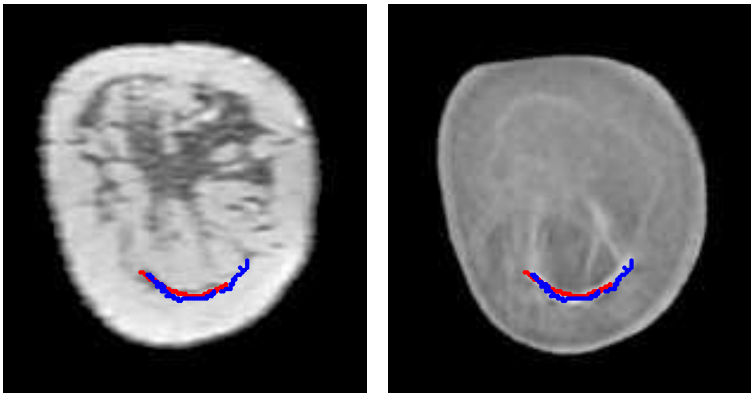

Figure 4: Result of the registration with strategy B. MRI (left) and USCT (right), each with markings of a connective tissue structure, which served as a basis for evaluation of the TRE. Blue denotes the surface points of the marking in USCT, red denotes the surface points of the marking in MRI. Note that both images show the same coronal slice from the 3D volumes.

While both strategies perform approximately equal with respect to their accuracy we assume less computational demand for strategy B as the forward problem of applying gravity to an unloaded configuration of the breast needs to be carried out only once, while for the inverse problem an iterative procedure with multiple applications of the forward problem is usually the method of choice. In the previous and present work we overcome the majority of the additional computational burden of the inverse problem by applying the iterative procedure only once with the optimal parameters. Yet, the optimization might result in even better parameters if also the iterative procedure is applied in each optimization step. For strategy B a similar trade-off was not necessary. Further analysis in future will test these hypotheses. Furthermore the strategy B could easily be extended by further boundary conditions, e.g. by modeling the MRI breast coils to cope for additional deformations when the breast is in contact with them.

In conclusion, we have developed the initial methods to compare two registration strategies in order to estimate the spatial correspondence between MRI and USCT and presented the preliminary results. The spatial correspondence allows to delineate corresponding tissue structures in both modalities in the same or nearby slices (Figures 3 and 4). It therefore can serve as a major tool for further analysis of USCT images, e.g. for human reader studies, quantitative analysis of sound speed and attenuation parameters similar to *Hopp et al.*[14] and for the development of computer aided detection (CADe) tools using classification of tissue types based on extracted image parameters.

References

[1] N. Duric, P. Littrup, P. Chandiwala-Mody, C. Li, S. Schmidt, L. Myc, O. Rama, L. Bey-Knight, J. Lupinacci, B. Ranger, A. Szczepanski, E. West: In-vivo imaging results with ultrasound tomography: Report on an ongoing study at the Karmanos Cancer Institute. Proc. SPIE Medical Imaging 7629 (2010), 76290M

[2] J. Wiskin, D. Borup, S. Johnson, M. Berggren, D. Robinson, J. Smith, J. Chen, Y. Parisky, J. Klock: Inverse Scattering and Refraction Corrected Reflection for Breast Cancer Imaging Proc. SPIE Medical Imaging 7629 (2010) 76290K

[3] N. Ruiter, M. Zapf, R. Dapp, T. Hopp, W. Kaiser, H. Gemmeke: First Results of Clinical Study with 3D Ultrasound Computer Tomography. Proc. IEEE Ultrasonics Symposium (2013), 651654

[4] T. Hopp, R. Dapp, M. Zapf, E. Kretzek, H. Gemmeke, N.V. Ruiter: Registration of 3D Ultrasound Computer Tomography and MRI for evaluation of tissue correspondences, Proc. SPIE Medical Imaging 9419 (2015), 941925

[5] T. Carter, C. Tanner, N. Beechey-Newman, D. Barratt, D. Hawkes: MR Navigated Breast Surgery: Method and Initial Clinical Experience. Medical Image Computing and Computer-Assisted Intervention MICCAI 2008, 5242 (2008) 356363.

[6] J.C. Bezdek: Pattern Recognition with Fuzzy Objective Function Algorithms. Norwell, MA, USA: Kluwer Academic Publishers (1981).

[7] T. Hopp, M. Zapf, N.V. Ruiter: Segmentation of 3D Ultrasound Computer Tomography Reflection Images using Edge Detection and Surface Fitting, Proc. SPIE Medical Imaging 9040 (2014), 904066

[8] Q. Fang, D.A. Boas: Tetrahedral mesh generation from volumetric binary and grayscale images. IEEE International Symposium on Biomedical Imaging: From Nano to Macro (2009) 11421145.

[9] A. F. Bower, Applied Mechanics of Solids. Taylor and Francis (2011)

[10] Dassault Systemes Simulia Corp.: ABAQUS Analysis User's Manual (2014)

[11] A.P. Cooper: On the anatomy of the breast. Longman, London (1840)

[12] A. Myronenko, A. Song: Intensity-based image registration by minimizing residual complexity, IEEE Transactions on Medical Imaging 29(11) (2010), 18821891

[13] P. Cotic Smole, C. Kaiser, J. Krammer, N.V. Ruiter, T. Hopp: A comparison of biomechanical models for MRI to digital breast tomosynthesis 3D registration. Proceedings MICCAI Workshop on Computational Biomechanics for Medicine XII (in press).

[14] T. Hopp, N. Duric, N.V. Ruiter: Image fusion of Ultrasound Computer Tomography volumes with X-ray mammograms using a biomechanical model based 2D/3D registration. Computerized Medical Imaging and Graphics 40 (2015), 170-181